Available online at www.sciencedirect.com
ScienceDirect
Fire Safety Journal 42 (2007) 115–126
FIRE SAFETY JOURNAL
www.elsevier.com/locate/firesaf

A parametric natural fire model for the structural fire design of multi-storey buildings

J. Zehfuss[a,*], D. Hosser[b]

[a]hhpberlin Fire Safety Engineers, Berlin, Germany
[b]Institute of Building Materials, Concrete Structures and Fire Protection (iBMB), Braunschweig University of Technology, Germany

Received 17 September 2004; received in revised form 10 July 2006; accepted 8 August 2006

Abstract

A parametric natural fire model is presented, which is derived on the basis of simulations with heat balance models for realistic natural design fires, taking into account the boundary conditions of typical compartments in residential and office buildings. These so-called iBMB parametric fire curves are formulated with the help of simplified empirical equations which can easily be used for structural fire design as part of a performance-based natural fire design concept. The iBMB parametric fire curves are checked and validated by comparison with results of different heat balance models and with published fire tests from different fire research laboratories. In addition, a natural fire test in a test room with ordinary office room furnishings has been performed which supports the parametric natural fire model presented here. The application of the iBMB parametric fire curves is demonstrated by means of an example.

Keywords: Simplified natural fire model; Structural fire design; Design fire; iBMB parametric fire curve

1. Introduction

Within a performance-based fire design concept the structural design should be based on a natural design fire which is representative for the boundary conditions of a given building. The "traditional way" of structural fire design using the ISO 834 temperature–time curve in many cases results in a design on the safe side causing unsatisfactory costs for fire protection measures, e.g. greater concrete cover of reinforced concrete elements, thicker cladding or over-dimensioning of steel elements, which entails economic as well as aesthetical disadvantages. In some cases the structural fire design with ISO 834 temperature–time curve can result in under-estimation of the thermal exposure.

In this paper a parametric natural fire model called *iBMB parametric fire curve* [1,2] is presented. It considers the actual boundary conditions of the fire compartment concerning fire load, ventilation conditions, geometry and thermal properties of the enclosure. The iBMB parametric fire curves are derived by heat balance simulations assuming a great number of natural designs fires by varying the above-mentioned parameters. The iBMB parametric fire curves are appropriate to describe the thermal action of natural fires in residential and office buildings including realistic room-to-room fire spread. Contrary to the Eurocode 1 parametric temperature–time curves, the iBMB parametric fire curves are directly derived from the rate of heat release defining the design fire.

Because of the connection between design fire and parametric fire curve, all events influencing the natural fire and resulting in a variation of the rate of heat release can be considered by the iBMB parametric fire curves. Thus the iBMB parametric fire curves can also be used to consider the occurrence of flashover, the breakage of windows with additional ventilation, a failure of the enclosure with loss of compartmentation or the effect of fire fighting and sprinkler systems. Whilst the iBMB parametric fire curves are valid for the structural fire design of each kind of structure, they offer the most benefit for steel structures.

*Corresponding author. Anciently: Institute of Building Materials, Concrete Structures and Fire Protection (iBMB), Braunschweig University of Technology, Germany.
E-mail address: j.zehfuss@hhpberlin.de (J. Zehfuss).

0379-7112/$ - see front matter © 2006 Elsevier Ltd. All rights reserved.
doi:10.1016/j.firesaf.2006.08.004

Nomenclature

A_f	floor area of fire compartment, m^2
A_t	total area of the enclosing components including openings, m^2
A_T	total area of the enclosing components without openings, m^2
A_w	area of ventilation openings, m^2
H_{net}	net calorific value, MJ/kg
O	opening factor ($A_w h_w^{1/2}/A_t$), $m^{1/2}$
Q	fire load, MJ
$\dot{Q}$	rate of heat release, MW
$\dot{Q}_{f,A}$	rate of heat release per unit area, fuel-controlled fire, MW/m^2
$\dot{Q}_{max}$	maximum rate of heat release, MW
$\dot{Q}_{max,f}$	maximum rate of heat release, fuel-controlled fire, MW
$\dot{Q}_{max,v}$	maximum rate of heat release, ventilation-controlled fire, MW
$\dot{Q}_v$	rate of heat release, ventilation-controlled fire, MW
T	temperature, °C
b	averaged thermal property of the enclosing components, $J/(m^2 s^{0.5} K)$
h_w	averaged height of the ventilation openings, m
$\dot{m}$	mass burning rate, kg/s
m_a	mass flow into the fire compartment, kg/s
$\dot{m}''$	mass burning rate per unit area, $kg/(m^2 s)$
q''	fire load density, MJ/m^2
r	stoichiometric fuel/air ratio, dimensionless
t	time, s
t_g	time of fire growth to 1 MW, s
χ	combustion efficiency, dimensionless

2. Natural fires in multi-storey buildings

2.1. Temperature–time curves

The standard temperature–time curve according to ISO 834 was developed in the 1930s summarising data from fires in residential, office and commercial buildings. The curve should cover most of the potential courses of fires in common buildings. As fire tests have shown, the maximum temperature of a natural fires can exceed the ISO-curve, but after the maximum it decreases again, whereas the ISO-curve rises continuously (Fig. 1).

Magnusson et al. [3] published curves describing the temperature development of natural fires on the basis of mass and energy balance equations. These curves have been incorporated into a Swedish standard and have served also as the basis for the parametric temperature–time curves of Eurocode 1-1-2 [4]. Latter can be applied to the structural fire design of small to medium rooms where a fully developed fire is assumed.

The parametric temperature–time curves of Eurocode 1-1-2, annex A in some cases provide an unrealistic temperature increase and decrease. One reason is that for fuel-controlled fires in residential and office buildings the maximum temperature is fixed at a fire duration of 20 min. For fire compartments with large openings and an enclosure with low thermal conductivity the Eurocode gives an extremely fast enhancement and decay of the temperature. For fire compartments with small openings and an enclosure with high thermal conductivity; however, an extremely slow decay of the temperature is assumed. The parametric temperature–time curves in Eurocode 1-1-2 [4] only describe the fully developed phase of the fire without considering the growth phase. Results of fire tests

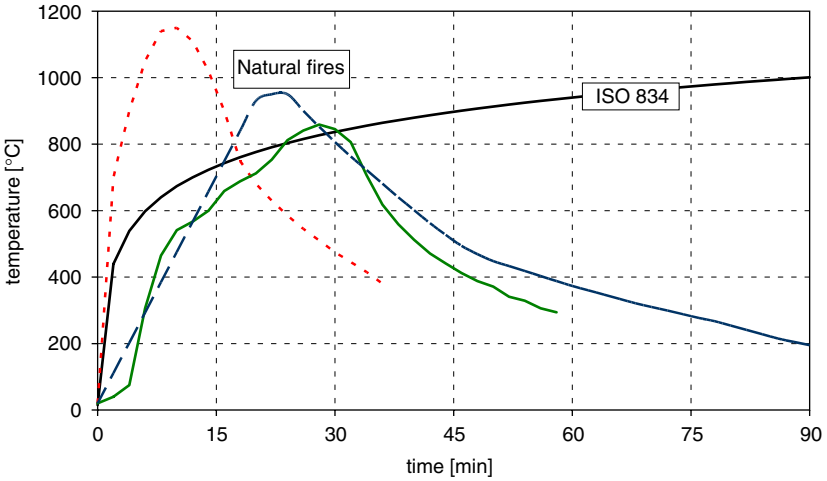

Fig. 1. Comparison of temperature–time curves in natural fires with ISO 834 standard fire.

with ordinary furnishings reveal that even in small fire compartments it can take some minutes to reach the fully developed fire from the initial fire. The most critical point is that the parametric temperature–time curves of Eurocode 1-1-2 annex A have no temporal connection with the rate of heat release of Eurocode 1-1-2 annex E.

This deficiency with respect to temperature increase and decrease will be clarified by comparing the parametric temperature–time curve according to Eurocode 1-1-2 with the recorded average temperature–time curve of the $NFSC_2$ fire test No. 2 at BRE [5] governed by fuel-controlled conditions (Fig. 2). Even more obvious is the discrepancy between the temporal course of the parametric temperature–time curve and the rate of heat release according to Eurocode 1-1-2 annex E. The latter achieves its maximum after 30 min and declines after 43 min. The parametric temperature–time curve and rate of heat release neither match each other nor are they temporally congruent.

A set of further procedures for the computation of temperature–time curves was developed during the last few years (e.g. [6–8]), a part of which is based on the above approach. Most of the proposals are derived from experimental results; therefore, their range of application is limited to compartments of dimensions and fire loads similar to those in the respective fire tests.

A more consistent way is to assume a realistic fire scenario, to define the resulting design fire and to compute on this basis the temperature–time curve using an established and validated fire simulation model. The range of application of such temperature–time curves is determined by the field of boundary conditions covered by the simulations.

2.2. Design fire

2.2.1. General

A performance-based structural fire design should be based on a realistic fire scenario which is described by a design fire taking into account the relevant boundary conditions (fire load, ventilation, geometry of fire compartment). The design fire is defined in terms of a rate of heat release, which can be used as input to most types of fire models for calculating important fire effects, e.g. temperatures and mass flow. This description is physically clearer and more general than temperature–time-curves [1]. The rate of heat release $\dot{Q}(t)$ is given by

$$\dot{Q}(t) = \dot{m}(t)\chi H_{\text{net}}. \tag{1}$$

The combustion efficiency χ is derived from experimental results, e.g. $\chi = 0.7$ for wooden fire loads [9]. The net calorific value can be taken as $H_{\text{net,wood}} = 17.3\,\text{MJ/kg}$ for wooden fire loads and furnishings [9,10]. The rate of heat release strongly depends on the ventilation conditions and a distinction is made between ventilation-controlled fires and fuel-controlled fires.

2.2.2. Ventilation-controlled fires

In small and medium-size rooms fully developed fires are frequently ventilation-controlled. They are governed by the size and shape of the ventilation openings (windows and doors). The mass flow rate through the ventilation openings can be assumed as

$$\dot{m}_a = 0.52\,A_w\sqrt{h_w}\,\text{kg/s}. \tag{2}$$

Being aware of the stoichiometric ratio ($r = 5.2\,\text{kg air/kg}$ burning material for wooden fire loads resp. furnishings), that is the required amount of air for the combustion per kg of burning material, the burning rate can be assumed as

$$\dot{m} = \frac{\dot{m}_a}{r} = \frac{0.52}{5.2}A_w\sqrt{h_w} = 0.1\,A_w\sqrt{h_w}\,\text{kg/s}. \tag{3}$$

Inserting Eq. (3) in Eq. (1) supplies the rate of heat release of a ventilation-controlled fire, which corresponds to annex E of Ref. [4]:

$$\dot{Q}_v = 0.1\,A_w\sqrt{h_w}\,\chi H_{\text{net}}\,\text{MW}. \tag{4}$$

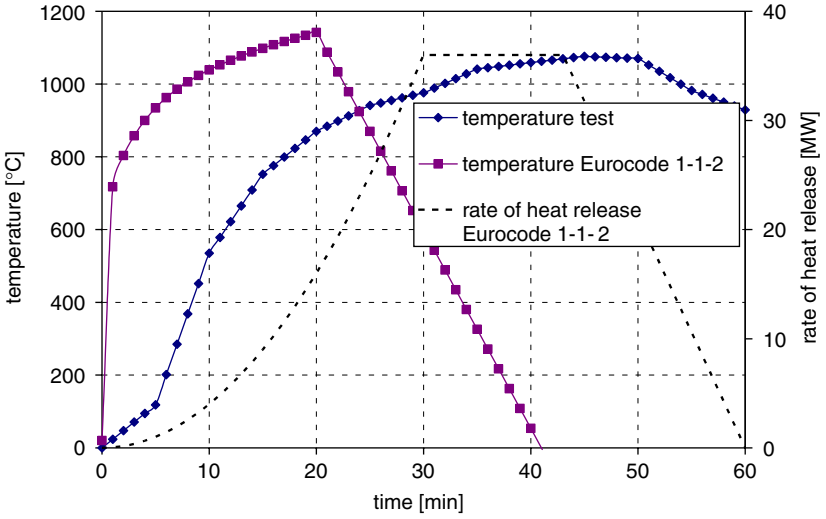

Fig. 2. Temperature–time curve and rate of heat release according to Eurocode 1-1-2 [4].

The maximum rate of heat release for residential and office buildings in case of a ventilation-controlled fire can be derived by inserting $\chi = 0.7$ and $H_{\text{net,wood}} = 17.3\,\text{MJ/kg}$ in Eq. (4):

$$\dot{Q}_{\max,v} = 1.21\, A_w \sqrt{h_w}\ \text{MW}. \tag{5}$$

2.2.3. Fuel-controlled fires

In large compartments fully developed fires are often fuel-controlled and the burning rate is primarily influenced by the area of the burning surface of the fire load. The rate of heat release can be defined as

$$\dot{Q}(t) = \dot{m}'' \cdot A_f(t) \cdot \chi \cdot H_{\text{net}}. \tag{6}$$

For wooden fire loads resp. furnishings the burning rate per unit area can be assumed as $\dot{m}'' = 0.02\,\text{kg/(m}^2\text{s)}$ [1]. Inserting $\chi = 0.7$ and $H_{\text{net,wood}} = 17.3\,\text{MJ/kg}$ in Eq. (6) the rate of heat release can be assumed as

$$\dot{Q}_{f,A}(t) = 0.02 \times 0.7 \times 17.3\, A_f(t) = 0.242\, A_f(t)\ \text{MW}. \tag{7}$$

In agreement with the investigation of [11] the maximum rate of heat release of multi-storey residential and office buildings in case of a fuel-controlled fire can be determined as

$$\dot{Q}_{\max,f} = 0.25\, A_f\ \text{MW}, \tag{8}$$

where by the maximum burning area $A_f(\text{m}^2)$ is assumed to be limited to the floor area of the fire compartment.

2.2.4. Rate of heat release

Fig. 3 illustrates the approach for the rate of heat release $\dot{Q}(t)$ [1,2]. For the growth phase of a fire in residential and office buildings the so-called t^2-approach finds general acceptance [4,11]:

$$\dot{Q}(t) = \dot{Q}_0 \left(\frac{t}{t_g}\right)^2, \tag{9}$$

where by $\dot{Q}_0 = 1.0\,\text{MW}$ and the time of fire growth—with a medium fire growth rate in residential and office buildings—can be assumed as $t_g = 300\,\text{s}$.

In the fully-developed fire the quadratic increase in the rate of heat release is replaced by a constant value which is taken as the minimum of the two rates of heat release, for fuel-controlled and ventilation-controlled fires predicted by Eqs. (5) and (8), respectively [1].

$$\dot{Q}_{\max} = \text{MIN}\left\{\dot{Q}_{\max,v};\ \dot{Q}_{\max,f}\right\}. \tag{10}$$

When 70% of the fire load is consumed, the rate of heat release decreases linearly until the fire load is completely burned [11].

2.3. iBMB parametric fire curves

2.3.1. General

The assessment of the natural fire is a substantial part of a performance-based fire design concept. For the derivation of iBMB parametric fire curves based on the approach of the rate of heat release, temperature–time curves were simulated with the zone model CFAST [12] for various boundary conditions vs. influencing factors [1,2]. Fig. 3 illustrates the qualitative shapes of the rate of heat release and the upper layer temperature computed with CFAST. The temporal link between the curves is evident. Both curves can be characterised by three distinctive points at the times t_1, t_2, t_3, where the slope of the curves is changing. From the beginning of the fire until t_1 the rate of heat release rises quadratically and the upper layer temperature increases rapidly. At t_1 the maximum rate of heat release is achieved and remains constant until t_2. After t_1 the upper layer temperature increases moderately. As 70% of the fire load is consumed at t_2, the rate of heat release drops off linearly. Achieving its maximum at t_2 hence the upper layer temperature declines. At t_3 the complete fire load is consumed and the rate of heat release decreases to 0.

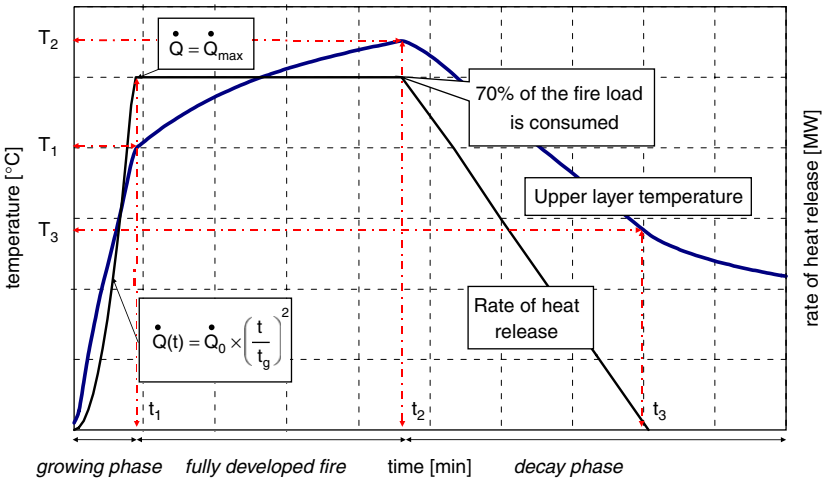

Fig. 3. Approach of the rate of heat release and the corresponding upper layer temperature (principle).

At this time the upper layer temperature–time curve bends and declines slower than before.

The times t_1, t_2, t_3 can be determined by the consideration of the functional course of the rate of heat release [1]. For the total description of the run of the upper layer temperature–time curve the associated temperatures T_1, T_2 and T_3 have to be ascertained (Fig. 3). Being aware of the characteristic times and temperatures, the course of the temperature can be described functionally as iBMB parametric fire curves. Thus, the iBMB parametric fire curves are a simplified description of the upper layer temperature–time curve of a natural fire. They can serve as a realistic thermal action for the structural fire design avoiding the application of sophisticated heat balance models.

For the derivation of the iBMB parametric fire curves the link between rate of heat release and the temperature–time curve is essential. Thus for a reference fire load density of $q'' = 1300\,\mathrm{MJ/m^2}$, which is taken as an upper value for residential and office buildings, parametric functions for the temperature–time curve were developed which consider the ventilation conditions, thermal properties of the enclosure and geometry of the compartment. For fire load densities less than the maximum, the maximum temperature is achieved accordingly earlier. The appropriate time can be ascertained from the rate of heat release function (Fig. 7).

2.3.2. Ventilation-controlled fires

The availability of oxygen controls the energy released in the compartment and, therefore, the resulting temperatures [13].

For the temperature development of ventilation-controlled fires, apart from the thermal properties of the enclosure, the opening factor O is predominant [7,14]. In Fig. 4 the maximum upper layer temperature T_2 at time t_2 (according to definition of Fig. 3) of ventilation-controlled fires for the reference fire load density of $q'' = 1300\,\mathrm{MJ/m^2}$ calculated with CFAST [12] is plotted against the factor $1/O$ for different thermal properties of the enclosure.

A regression analysis for the upper layer temperatures T_1, T_2 and T_3 of ventilation-controlled fires provides the following functions for the reference fire load density of $q'' = 1300\,\mathrm{MJ/m^2}$ [1]:

$$T_1 = -8.75 \times 1/O - 0.1\,b + 1175\,^{\circ}\mathrm{C}, \tag{11}$$

$$T_2 = (0.004\,b - 17) \times 1/O - 0.4\,b + 2175^{\circ}\mathrm{C} \leqslant 1340^{\circ}\mathrm{C}, \tag{12}$$

$$T_3 = -5.0 \times 1/O - 0.16\,b + 1060\,^{\circ}\mathrm{C}, \tag{13}$$

with the opening factor

$$O = A_w\sqrt{h_w}/A_t\ \mathrm{m}^{1/2}. \tag{14}$$

2.3.3. Fuel-controlled fires

For the temperature development of fuel-controlled fires, apart from the heat loss out of openings and through the boundaries, the heat released by the fire source is the most important factor [15]. In Fig. 5 the maximum upper layer temperature T_2 at time t_2 (according to definition of Fig. 3) of fuel-controlled fires for the reference fire load density of $q'' = 1300\,\mathrm{MJ/m^2}$ calculated with CFAST [12] is plotted against the factor k (according to Eq. (18)). The linear correlation between k and the maximum temperature T_2 for $k < 0.04$ is indicated by the continuous line.

Performing a regression analysis for the upper layer temperatures T_1, T_2 and T_3 of fuel-controlled fires the following functions can be determined for the reference fire load density of $q'' = 1300\,\mathrm{MJ/m^2}$ [1]:

$$T_1 = 24\,000\,k + 20\,^{\circ}\mathrm{C} \quad \text{for } k \leqslant 0.04 \quad \text{and}$$
$$T_1 = 980\,^{\circ}\mathrm{C} \quad \text{for } k > 0.04, \tag{15}$$

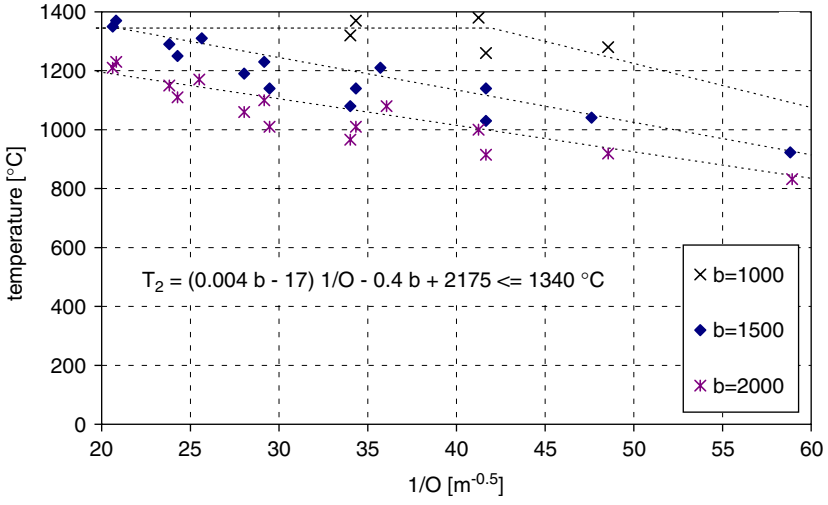

Fig. 4. Maximum temperatures T_2 of ventilation-controlled fires ($q'' = 1300\,\mathrm{MJ/m^2}$) in dependence of the inverse opening factor $1/O$ for different thermal properties of the enclosure.

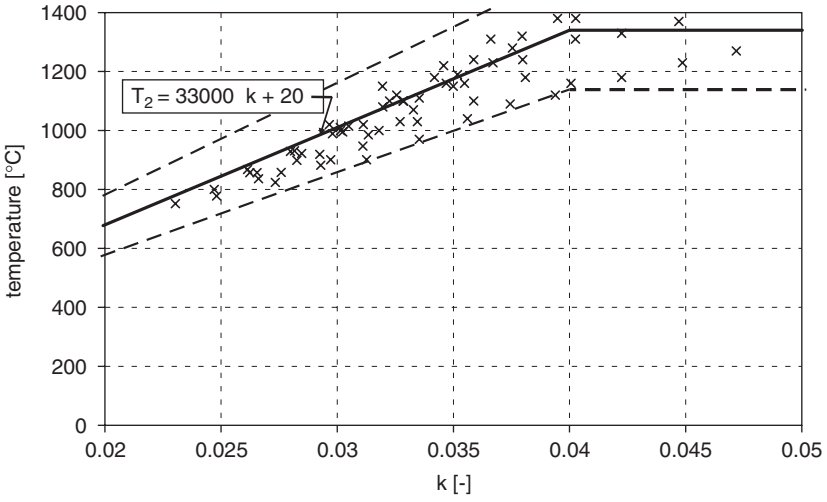

Fig. 5. Maximum temperatures T_2 of fuel-controlled fires ($q'' = 1300\,\mathrm{MJ/m^2}$) in dependence of factor k.

$$T_2 = 33\,000\,k + 20\,^{\circ}\mathrm{C} \quad \text{for } k \leqslant 0.04 \quad \text{and}$$
$$T_2 = 1340\,^{\circ}\mathrm{C} \quad \text{for } k > 0.04, \tag{16}$$

$$T_3 = 16\,000\,k + 20\,^{\circ}\mathrm{C} \quad \text{for } k \leqslant 0.04 \quad \text{and}$$
$$T_3 = 660\,^{\circ}\mathrm{C} \quad \text{for } k > 0.04, \tag{17}$$

with

$$k = \left(\frac{\dot{Q}^2}{A_w \sqrt{h_w}\, A_T\, b} \right)^{1/3}. \tag{18}$$

2.3.4. Functional description

The functional form of the iBMB parametric fire curves between the characteristic points can be described by three sections (Fig. 6). In Section 1 ($0 \leqslant t \leqslant t_1$) the temperature rises quadratically:

$$T = \frac{(T_1 - T_0)}{t_1^2}\, t^2 + T_0, \tag{19}$$

with time in minutes and temperatures in °C, thus T_0 is the ambient temperature, usually 20 °C.

The more moderate slope within Section 2 ($t_1 < t \leqslant t_2$) can be described by a square root function:

$$T = (T_2 - T_1)\sqrt{(t - t_1)/(t_2 - t_1)} + T_1, \tag{20}$$

likewise the decrease of temperature within Section 3 ($t > t_2$):

$$T = (T_3 - T_2)\sqrt{(t - t_2)/(t_3 - t_2)} + T_2. \tag{21}$$

Fig. 6 shows the graphical illustration of the functions describing the iBMB parametric fire curves for the reference fire load density of $q'' = 1300\,\mathrm{MJ/m^2}$.

On the basis of the iBMB parametric fire curve for the reference fire load density $q'' = 1300\,\mathrm{MJ/m^2}$, the curves for other fire load densities $q''_x \leqslant 1300\,\mathrm{MJ/m^2}$ can be determined. The fire load Q_x is ascertained by multiplying the fire load density q''_x and the fire area A_f:

$$Q_x = q_x\, A_f. \tag{22}$$

The increasing branch of the iBMB parametric fire curve is independent of the fire load density until the maximum temperature is achieved. The time $t_{2,x}$ where the maximum temperature $T_{2,x}$ appears, depends on the fire load and can be ascertained directly from the approach of the rate of heat release. In reference to Fig. 3 with

$$Q_1 = \dot{Q}_0 \int_0^{t_1} \left(\frac{t}{t_g} \right)^2 \mathrm{d}t, \tag{23}$$

and

$$Q_{2,x} = 0.7\, Q_x - Q_1, \tag{24}$$

for $Q_1 \leqslant Q_{2,x}$ can be obtained:

$$t_{2,x} = t_1 + \frac{(0.7\, Q_x) - \dot{Q}_0 \left(t_1^3 / \left(3\, t_g^2 \right) \right)}{\dot{Q}_{\max}}. \tag{25}$$

For small fire load densities q''_x with $Q_1 \geqslant 0.7\, Q_x$ $t_{2,x}$ is assumed as

$$t_{2,x} = \sqrt[3]{0.7\, Q_x\, 3\, t_g^2}. \tag{26}$$

The associated temperature $T_{2,x}$ is ascertained by inserting $t = t_{2,x}$ in Eq. (20):

$$T_{2,x} = (T_2 - T_1)\sqrt{(t_{2,x} - t_1)/(t_2 - t_1)} + T_1. \tag{27}$$

For different fire load densities the temperatures $T_{3,x}$ at time $t_{3,x}$ are in line with a logarithmic function through $(t = 0; T_0)$ and $(t_3; T_3)$:

$$T_{3,x} = \left(T_3 / \log_{10}(t_3 + 1) \right) \log_{10}\left(t_{3,x} + 1 \right). \tag{28}$$

The decreasing branch of the iBMB parametric fire curve in Section 3 with $q''_x < 1300\,\mathrm{MJ/m^2}$ can be ascertained by

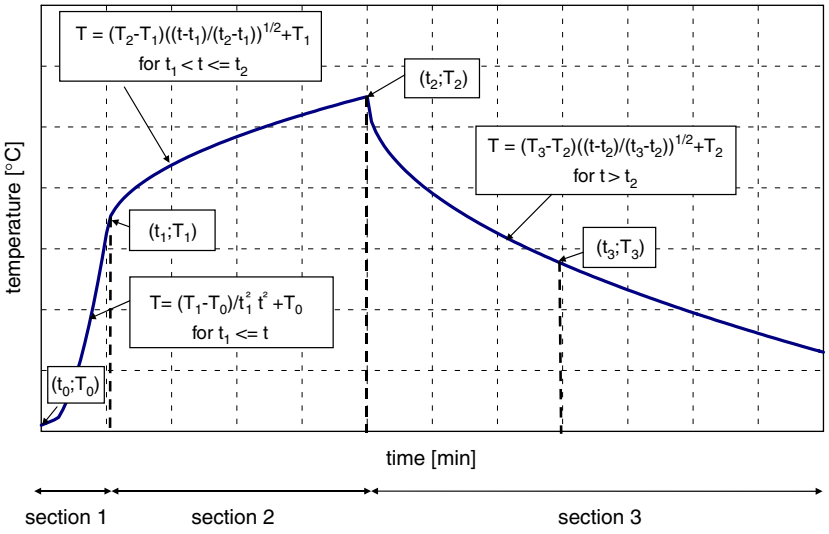

Fig. 6. Mathematical description of the iBMB parametric fire curves in 3 sections.

substituting in Eq. (21):

$$T = \left(T_{3,x} - T_{2,x}\right)\sqrt{(t - t_{2,x})/(t_{3,x} - t_{2,x})} + T_{2,x}. \tag{29}$$

2.3.5. Flashover

The critical rate of heat release for the incidence of flashover can be calculated according to the method of Thomas [9]. Thomas uses the energy balance of the upper layer for the derivation of the critical rate of heat release $\dot{Q}_{\mathrm{fo}}$ for flashover, which can be determined by

$$\dot{Q}_{\mathrm{fo}} = 0.0078\, A_T + 0.378\, A_w\sqrt{h_w}\ \mathrm{MW}. \tag{30}$$

For the development of the iBMB parametric fire curves this expression is applied to estimate the time to flashover, when the rate of heat release reaches its maximum value:

$$t_{1,\mathrm{fo}} = \sqrt{t_g^2\,\dot{Q}_{\mathrm{fo}}}. \tag{31}$$

If the time $t_{1,\mathrm{fo}}$ is less than the time t_1, Eq. (30) has to be taken into account. In case of $t_{1,\mathrm{fo}} \geqslant t_1$, which can be expected especially for small compartments, the rate of heat release increases quickly to the maximum.

The fire load consumed until the time to flashover is determined as

$$Q_{1,\mathrm{fo}} = \frac{t_{1,\mathrm{fo}}^3}{3\,t_g^2}. \tag{32}$$

By inserting $Q_{1,\mathrm{fo}}$ instead of Q_1 and $t_{1,\mathrm{fo}}$ instead of t_1 the total development of the fire can be described [1].

2.3.6. Room cells

With the iBMB parametric fire curves presented here, successive fire spread in compartments which are subdivided into so-called room cells can be presented in a simplified approach. In office buildings the internal walls between the rooms (cells) are often light partitions which have a low fire rating and no fire classification. The cell walls prevent unobstructed fast fire spread. Thus a growing fire successively spreads from one room cell to the next one until the whole storey is involved in the fire.

The structural fire design of buildings with cell constructions leads to an overestimation of the fire action if the delaying effect of the cell walls is not considered. The standard fire design (ISO 834), the design with the parametric temperature–time curves of [4], and the method of equivalent time of fire exposure according to [4], annex F assume an unhindered fire spread over the whole compartment. The simplified approach of the design fire presented in this contribution allows the consideration of a successive spreading fire.

For considering the fire spread from one cell to the adjacent cell the failure criterion of the partition (e.g. EI-criteria of EN 13501-2) has to be known. In many cases a critical temperature can be determined and the failure time can be determined by heat transfer simulations. Alternatively, the principle of equivalent time of fire duration can be used to derive the failure criteria from the failure time under standard fire exposure.

Taking into account successive fire spread, the rate of heat release has to be adapted to the governing boundary conditions. After the breakthrough from the cell of fire initiation, the rate of heat release is calculated for the enlarged room with possibly varied fire load density, larger openings and varied thermal properties of the enclosure. Depending on the construction of the cell walls, the fire spreads to two, three or more cells. With the growing fire, the failure times of the cell walls decrease, thus after the second breakthrough of the cell a fully developed fire in the whole compartment (storey) can be assumed (Figs. 7 and 8).

For the validation of this simplified approach a comparative calculation with the CFD-model FDS [16]

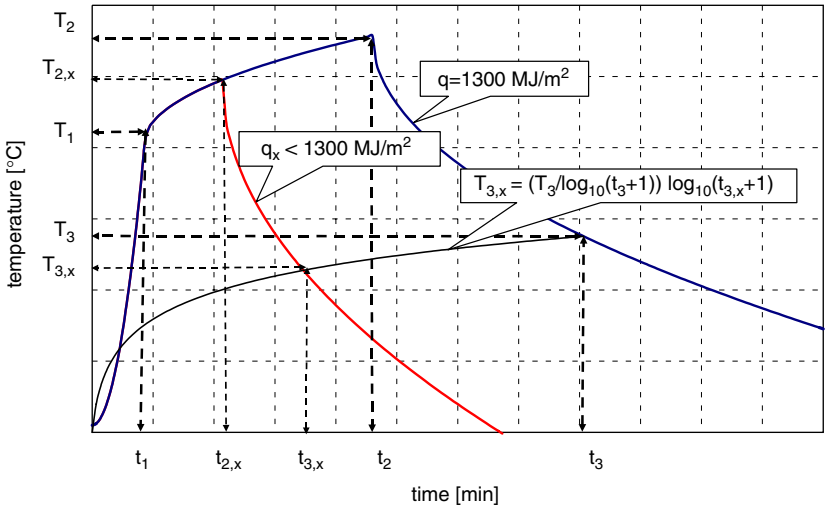

Fig. 7. Determination of the temperatures $T_{2,x}$ and $T_{3,x}$.

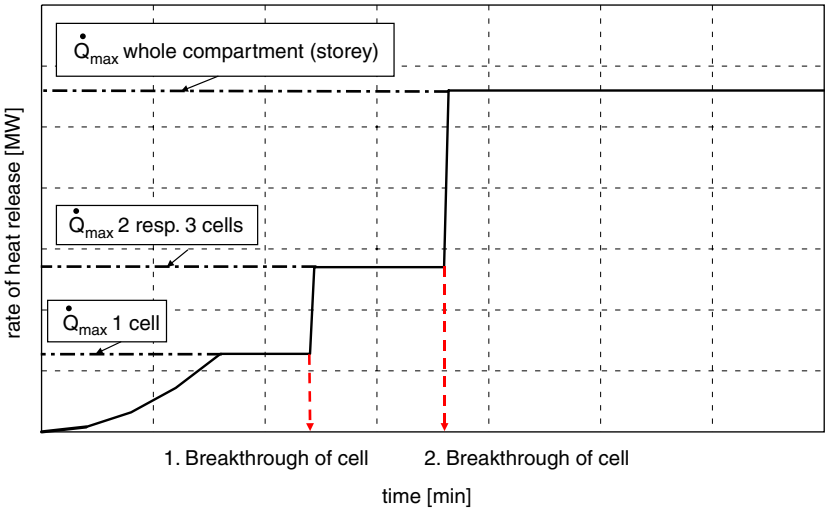

Fig. 8. Development of the rate of heat release in case of successive fire spread in a building containing a cell construction (qualitative).

was carried out where the development of the rate of heat release and the temperature for successive fire spread is investigated. For the cell of fire origin the rate of heat release is defined according to the approach given in Section 2.2.4. It is assumed that after 10 min the critical temperature of the cell wall between cells 1 and 2 is achieved and the wall fails (Fig. 9).

In the adjacent cell the fire loads are modelled as objects whose thermo-physical properties such as ignition temperature, density and heat of combustion are given. The ignition, the rate of burning and heat release of the objects are simulated by the combustion model of [16]. In Fig. 10 the rate of heat release according to the simplified approach is compared to the rate of heat release resulting from the CFD-simulation. Both curves run nearly congruent apart from a peak at the breakthrough of the cells after 10 min. This is the point where in the CFD-simulation the released energy suddenly increases due to the rapid ignition of the fire loads in cell 2.

Fig. 11 depicts the iBMB parametric fire curve and the temperature–time curve simulated with FDS which is determined by averaging the values of the thermocouples in the upper half of the total room. It is clear that the temperature–time curve bends due to the breakthrough of the cell and becomes consistent with the changed boundary conditions of the fire compartment formed by the two cells. After the cell breakthrough the iBMB parametric fire curve and the temperature–time curve simulated with FDS deviate only slightly.

2.3.7. *Validation of the iBMB parametric fire curves*

By a comprehensive validation it was shown that the iBMB parametric fire curves can realistically follow the temperature development of natural fires. The validation was carried out in three steps by means of

- a wide range of comparative calculations with heat balance models,

- comparative simulations of published fire tests from different fire research laboratories,
- performing a natural room fire test with ordinary office room furnishings.

The integral of the iBMB parametric fire curve vs. upper layer temperature–time curve after 30, 60 and 90 min serves as validation criteria. This integral represents the flow of energy into the structural elements. Another validation criterion is the maximum temperature.

In the first step for several room configurations with varying dimensions, openings and fire load densities the iBMB parametric fire curves have been calculated and compared with temperature–time curves computed with heat balance models whose aptitude can be implied according to international round robin tests. It has been shown that the iBMB parametric fire curves can match the computed temperature–time curves with good correlation [1].

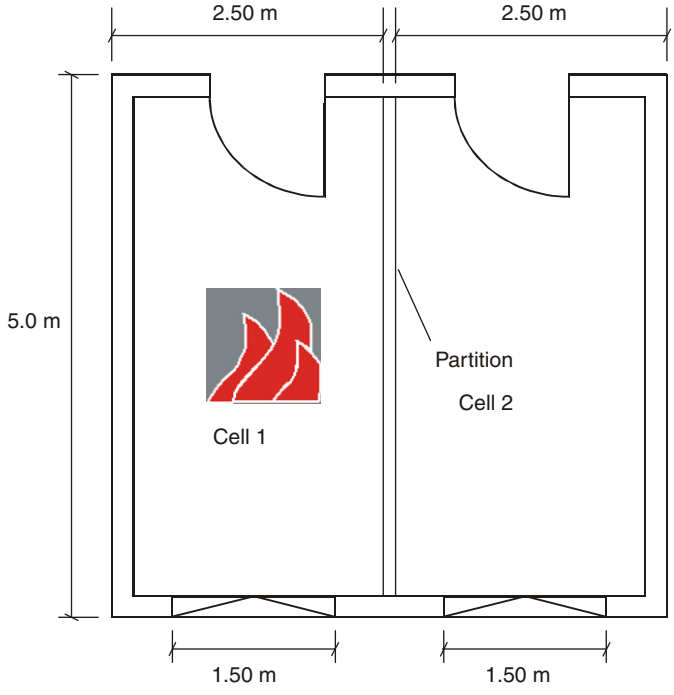

Fig. 9. Plan view of an office with room cells.

The second step includes validation by means of several published fire tests in compartments with varying dimensions, fire loads and openings carried out by different test laboratories. For each fire test the temperature–time curve was calculated by the iBMB method, with zone models [12] and [17], and with the simplified methods [4,6–8]. Fig. 12 illustrates the comparison of the maximum temperatures in the tests (horizontal axis) with the maximum temperatures calculated by the different methods (vertical axis). The bisecting line displays the equality of measured and calculated maximum temperatures. Most results calculated by the iBMB parametric fire curves are within the 15 percent bounds given by the dotted lines, only few of them are beyond the upper bound on the safe side. The scatter of the results of the iBMB parametric fire curve is smaller than that of the other methods.

For the third step of validation a natural fire test was carried out in a compartment with typical dimensions of an office room ($W/D/H = 3.60/3.60/2.60$ m) [1]. The fire load density was $q'' = 468\ \mathrm{MJ/m^2}$ containing furnishings, hardware, folders and papers. The single, relatively small opening ($b_w = 0.70$ m; $h_w = 2.60$ m) caused ventilation-controlled conditions during the fully developed fire. For supplying a wide database of a natural fire in an office room, the rate of heat release, mass loss rate, temperatures at several levels and the pressure profile in the opening were measured. Fig. 13 shows the comparison of recorded and calculated temperature–time curve in the upper layer [1]. The iBMB parametric fire curve fits well to the recorded test temperature–time curve and follows the progress of temperature as well as the zone models CFAST [12] and OZONE [17].

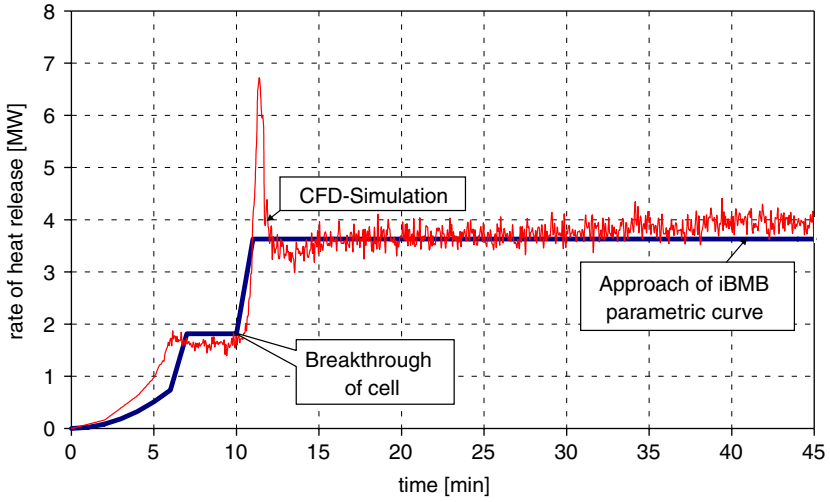

Fig. 10. Comparison of the rate of heat release according to the approach of the iBMB parametric curves and the simulation result of FDS [16].

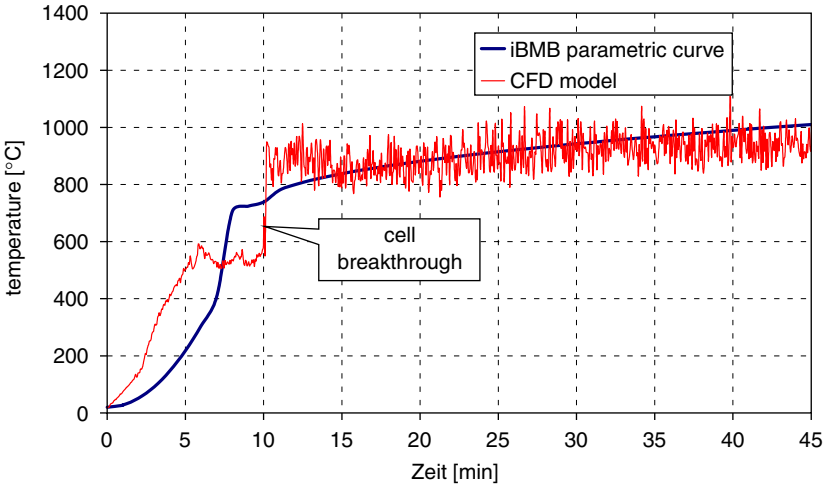

Fig. 11. Comparison of iBMB parametric curve and temperature–time curve simulated with FDS [16].

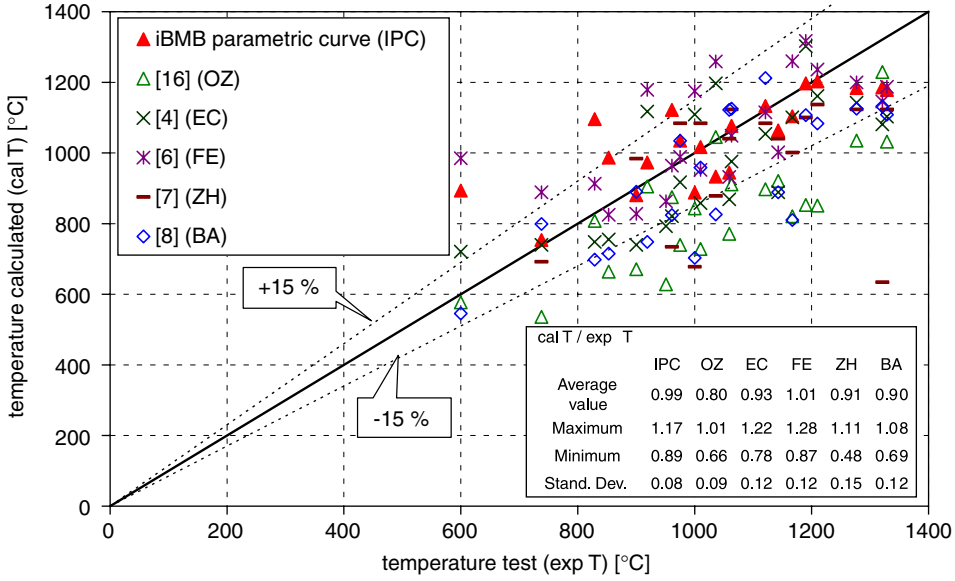

Fig. 12. Comparison of maximum temperatures measured in different fire tests and those calculated with different methods (criterion T_{max}).

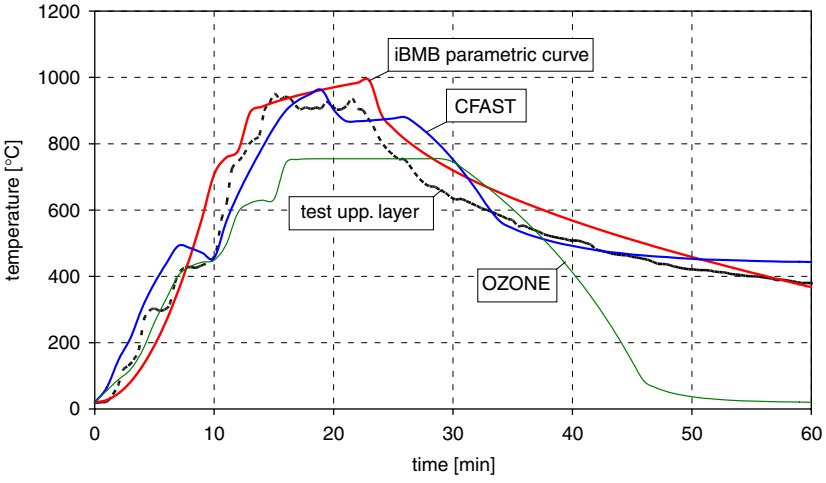

Fig. 13. Comparison of temperature–time curves measured in a natural room fire test with ordinary office room furnishings and those calculated with different methods [1].

3. Example office fire

By means of an example the application of the iBMB parametric fire curve is demonstrated.

Office fire compartment (area $A_f = 16\,\mathrm{m}^2$, height $H = 3\,\mathrm{m}$, area of openings $A_w = 8\,\mathrm{m}^2$, averaged height of openings $h_w = 2.50\,\mathrm{m}$):

ventilation factor	$A_w\sqrt{h_w} = 12.65\,\mathrm{m}^{3/2}$
opening factor	$O = 0.158\,\mathrm{m}^{1/2}$
fire load density (resp. [4])	$q'' = 511\,\mathrm{MJ/m}^2$
total fire load	$Q_{511} = 8176\,\mathrm{MJ}$
averaged thermal property of enclosure	$b = 1500\,\mathrm{J/(m}^2\mathrm{s}^{0.5}\mathrm{K)}$
total area of enclosing components (incl. openings)	$A_t = 80.0\,\mathrm{m}^2$
total area of enclosing components (without openings)	$A_T = 72.0\,\mathrm{m}^2$

rate of heat release

$$\dot{Q}_{\max} = \mathrm{MIN}(\dot{Q}_{\max,v}; \dot{Q}_{\max,f}) = \mathrm{MIN}(1.21\,A_w\sqrt{h_w}; 0.25\,A_f) = \mathrm{MIN}(15.31; 4.0),$$

$$\dot{Q}_{\max} = \dot{Q}_{\max,f} = 4.0\ \mathrm{MW} \Rightarrow \text{fuel-controlled fire},$$

$$Q = q\,A_f = 1300 \times 16.0 = 20,800\ \mathrm{MJ},$$

$$t_1 = 600\ \mathrm{s} = 10\ \mathrm{min}; \quad Q_1 = 800\ \mathrm{MJ},$$

$$Q_2 = 13\,760\ \mathrm{MJ}; \quad t_2 = 4040\ \mathrm{s} \approx 67\ \mathrm{min},$$

$$Q_3 = 6240\ \mathrm{MJ}; \quad t_3 = 7160\ \mathrm{s} \approx 119\ \mathrm{min},$$

$$Q_{2,511} = 4923\ \mathrm{MJ}; \quad t_{2,511} = 1831\ \mathrm{s} \approx 31\ \mathrm{min},$$

$$Q_{3,511} = 2453\ \mathrm{MJ}; \quad t_{3,511} = 3057\ \mathrm{s} \approx 51\ \mathrm{min},$$

$$k = (\dot{Q}^2_{\max}/(A_w\sqrt{h_w} \cdot A_T \cdot b))^{1/3} = 0.0227,$$

$$T_{1,f} = 24\,000\,k + 20 = 565\ ^\circ\mathrm{C},$$

$$T_{2,f} = 33\,000\,k + 20 \leqslant 1340\ ^\circ\mathrm{C} \Rightarrow T_2 = 769\ ^\circ\mathrm{C},$$

$$T_{3,f} = 16\,000\,k + 20 = 383\ ^\circ\mathrm{C},$$

$$T_{2,511} = 689\ ^\circ\mathrm{C},$$

$$T_{3,511} = 316\ ^\circ\mathrm{C}.$$

Fig. 14 illustrates the iBMB parametric fire curve compared to the upper layer temperature simulated with the fire model CFAST [12] and to ISO 834 temperature–time curve. iBMB parametric fire curve and CFAST upper layer temperature–time curve yield a good correlation.

For the actual boundary conditions the ISO 834 temperature–time curve overestimates the temperatures of the natural fire in the office and leads to an inefficient design of components.

4. Conclusion and outlook

The structural fire design for residential and office buildings can be optimised by considering the realistic development of the natural fire. Usually the structures are designed according to ISO 834 standard fire which can lead to inadequate fire protection measures. For a performance-based structural fire design the fire scenario itself needs detailed discussion and a more realistic description. The iBMB parametric fire curves presented in this paper include the growing and the decay phase of a fire. Contrary to other simplified natural fire models as e.g. the parametric temperature–time curves of Eurocode 1-1-2 the iBMB parametric fire curves distinguishes two key aspects. They can consider the actual ventilation conditions and they are

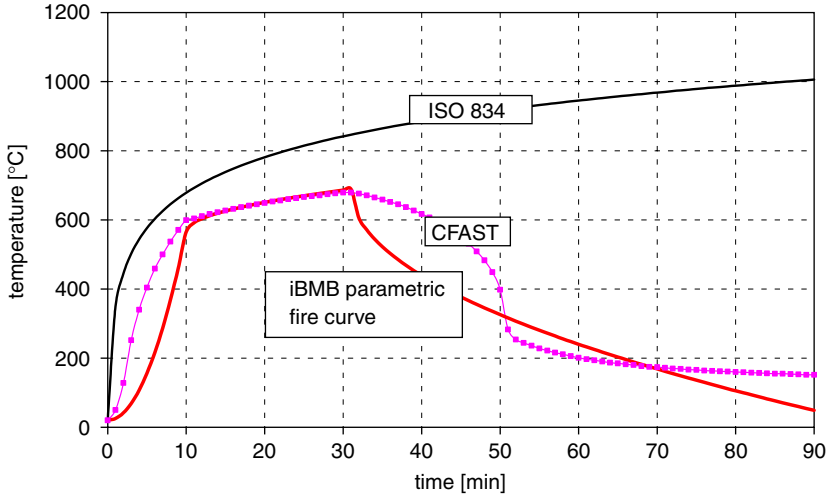

Fig. 14. Comparison of iBMB parametric fire curve and upper layer temperature–time curve (CFAST) of an office fire with ISO 834 temperature–time curve.

based on a realistic design fire which entails a temporally congruence with the rate of heat release. Due to the link to the rate of heat release with iBMB parametric fire curves the modification of boundary conditions in a fire caused by e.g. flashover, failure of compartmentation or fire fighting can be considered.

The iBMB parametric fire curves can serve as a basis for advanced calculation methods (according to the Eurocodes) for structural fire design. Whilst the simplified natural fire model can be applied to all types of structures, the most benefit is provided for the design of steel structures. Apart from the realistic fire development the consideration of load redistributions in the overall structure also provides advantages in fire safety design [18]. As shown in [1] the consideration of both: realistic fire development and the overall structural behaviour can lead to an efficient and aesthetical construction with unprotected steel components.

References

[1] Zehfuß J. Bemessung von Tragsystemen mehrgeschossiger Gebäude in Stahlbauweise für realistische Brandbeanspruchung. Dissertation Braunschweig University of Technology, 2004.
[2] Hosser D, Zehfuß J. Behaviour of structural systems exposed to natural fires considering the failure of substructures and repair. Third international workshop structures in fire, Ottawa, May 2004.
[3] Magnusson SE, et al. Temperature–time curves of complete process of fire development. Bulletin 16. Lund, Sweden: Institute of Technology; 1970.
[4] prEN 1991-1-2; Eurocode 1 part 1-2. Actions on structures: general actions—actions on structures exposed to fire. Second draft, March 2001.
[5] Schleich JB, et al. Natural fire safety concept full scale tests, implementation in the eurocodes and development of an userfriendly design tool. Technical report no. 6, period from 01.01.2000–30.06.2000. CEC agreement 7210-PA/PB/PC/PD/PE/PF/PR-060. Esch/Alzette, 2000.
[6] Feasey R, Buchanan B. Post-flashover fires for structural design. Fire Saf J 2002;37:83–105.
[7] Zhongcheng M, Mäkeläinen P. Parametric temperature–time curves of medium compartment fires for structural design. Fire Saf J 2000;34:361–75.
[8] Barnett CR. BFD curve: a new empirical model for fire compartment temperatures. Fire Saf J 2002;37:437–63.
[9] Society of Fire Protection Engineers, National Fire Protection Association, editor. The SFPE handbook of fire protection engineering. Quincy, MA, USA, 1990.
[10] DIN 18230 Teil 3 (German Standard). Baulicher Brandschutz im Industriebau; Rechenwerte. Berlin: Beuth Verlag; 2002.
[11] Schleich JB, et al. Competitive steel buildings through natural fire safety concept: draft final report: CEC agreement 7210-SA/125, 1999.
[12] Portier RW, Reneke PA, Jones WW, Peacock RD. A user's guide for CFAST, version 2.01. NISTR4985, National Institute of Standards and Technology. Gaithersburg, MD, USA: Building and Fire Research Laboratory; 1994.
[13] Bryl S, et al. Simulation von Modellbränden in Räumen. Alternative Methode zur Beurteilung von Brandschutzmassnahmen, Schweizer Ingenieur und Architekt, 1987. p. 391–402.
[14] Law M. A basis for the design of fire protection of building structures. Struct Eng 1983;61:25–33.
[15] McCaffrey BJ, Quintierre JG, Harkleroad MF. Estimating room fire temperatures and the likelihood of flashover using fire test data correlations. Fire Technol 1981;17:98–119.
[16] McGrattan KB, et al. Fire dynamics simulator (Version 3), user's guide: National Institute of Standards and Technology. US Department of Commerce; 2002.
[17] Cadorin JF, Franssen JM, Pintea D. The design fire tool OZONE, V 2.0—theoretical description and validation on experimental fire tests, 1st draft, 11.06.2001. Liege, University, 2001.
[18] Bailey C, et al. The behaviour of multi-storey steel framed buildings in fire, a European joint research programme. Swinden: Technology Centre; 1998.